Draft version April 30, 2007
Preprint typeset using LaTeX style emulateapj v. 6/22/04

THE ORBIT OF THE QUADRUPLE STAR SYSTEM 88 TAU A FROM PHASES DIFFERENTIAL ASTROMETRY AND RADIAL VELOCITY

Benjamin F. Lane[1], Matthew W. Muterspaugh[2,7], Francis C. Fekel[3], Michael Williamson[3], Stanley Browne[2], Maciej Konacki[4], Bernard F. Burke[1], M. M. Colavita[5], S. R. Kulkarni[6], M. Shao[5],

Draft version April 30, 2007

ABSTRACT

We have used high precision differential astrometry from the Palomar High-precision Astrometric Search for Exoplanet Systems (PHASES) project and radial velocity measurements covering a timespan of 20 years to determine the orbital parameters of the 88 Tau A system. 88 Tau is a complex hierarchical multiple system comprising a total of six stars; we have studied the brightest 4, consisting of two short-period pairs orbiting each other with an ∼18-year period. We present the first orbital solution for one of the short-period pairs, and determine the masses of the components and distance to the system to the level of a few percent. In addition, our astrometric measurements allow us to to make the first determination of the mutual inclinations of the orbits.
Subject headings: techniques:interferometric–star:88 Tau

1. INTRODUCTION

88 Tau (HD 29140, HR 1458, HIP 21402) is a bright ($m_V = 4.25, m_K = 3.69 \pm 0.25$; Skrutskie et al. 2006), nearby ($\sim$ 50pc) hierarchical sextuple stellar system (Tokovinin 1997). The A component contains a pair of systems(designated Aa and Ab) in an $\sim$ 18-year period (Balega et al. 1999) orbit that has been resolved by speckle interferometry (McAlister et al. 1987). The Aa component is a known spectroscopic binary system ($P \sim 3.57$-day) orbit, with a composite spectral type of A5m(Cowley et al. 1969). In previous work it had been noted (Burkhart & Coupry 1988) that the A system was likely complex, with possibly as many as 5 components. In this work we have determined that, like the Aa component, the Ab component is a double-lined binary with a period of 7.89 days. Finally, there is a common-proper-motion companion, labeled B, located ∼69 arcseconds away from the A system; it, too, is known to be a binary (Tokovinin & Gorynya 2001). For clarity we provide a schematic of this complex system in Figure 1.

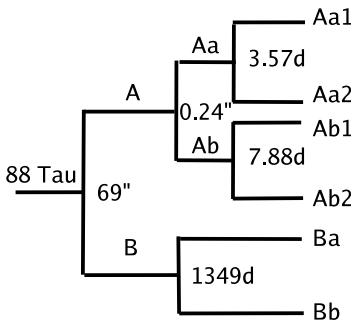

Fig. 1.— A schematic diagram of the 88 Tau system.

There are several reasons why multiple stellar systems such as 88 Tau merit attention: first, binary orbits make it possible to accurately measure stellar masses and distances, while the larger number of presumably co-eval stars allows one to impose the additional constraint that any given model must accurately match all of the stars. Second, as outlined in Sterzik & Tokovinin (2002), the relative orientations of the orbital angular momenta allow one to constrain the properties of the cloud from which the stars are thought to have formed, as well as the subsequent dynamical decay process. Despite their value, observational problems have limited the number of triple or higher-order systems with accurately measured orbits to fewer than 10. Given their hierarchical nature it is often the case that either the close system is unresolvable or the outer system has an impractically long orbital period.

With the advent of long-baseline stellar interferometry, and more recently phase-referenced long-baseline interferometric astrometry (Lane & Muterspaugh 2004) capable of 10–20 μ-arcsecond astrometric precision between pairs of stars with separations in the range 0.05–1 arcsecond, it has become possible to resolve the orbital motion of several interesting multiple systems (Muterspaugh et al. 2006b,a). Here we report on astrometric and radial velocity measurements of the 88 Tau system, which allow us to constrain the orbits of the 3.57-day, 7.8-day and 18-year components with improved precision, and for the first time provide a relative orientation of the orbits as well as component masses.

Astrometric measurements were made using the Palomar Testbed Interferometer (Colavita et al. 1999) as part of the Palomar High-precision Astrometric Search for Exoplanet Systems (PHASES) program (Muterspaugh et al. 2006c). The Palomar Testbed Interferometer is located on Palomar Mountain near San Diego, CA. It was

[1] MIT Kavli Institute for Astrophysics and Space Research, MIT Department of Physics, 70 Vassar Street, Cambridge, MA 02139
[2] University of California, Space Sciences Laboratory, 7 Gauss Way, Berkeley, CA 94720-7450
[3] Center of Excellence in Information Systems, Tennessee State University, 3500 John A. Merritt Blvd, Box 9501, Nashville, TN 37209
[4] Nicolaus Copernicus Astronomical Center, Polish Academy of Sciences, Rabianska 8, 87-100 Torun, Poland
[5] Jet Propulsion Laboratory, California Institute of Technology, 4800 Oak Grove Dr., Pasadena, CA 91109
[6] Division of Physics, Mathematics and Astronomy, 105-24, California Institute of Technology, Pasadena, CA 91125
[7] Townes Fellow

developed by the Jet Propulsion Laboratory, California Institute of Technology for NASA as a testbed for interferometric techniques applicable to the Keck Interferometer and the Space Interferometry Mission (SIM). It operates in the J (1.2 μm), H (1.6 μm), and K (2.2 μm) bands and combines starlight from two out of three available 40 cm apertures. The apertures form a triangle with 86 and 110 m baselines.

2. OBSERVATIONS & MODELS

2.1. *PHASES Astrometry*

88 Tau A was successfuly observed with PTI on 29 nights in 2004–2006 using the phase-referenced fringe-scanning mode (Lane & Muterspaugh 2004) developed for high-precision astrometry; the data was reduced using the algorithms described therein, together with the modifications described in Muterspaugh et al. (2005).

The obtained differential astrometry is listed in Table 1. Note that the astrometry on any single night is essentially that of a single-baseline interferometer, yielding a very small error in the direction aligned with the baseline, but limited to the effect of Earth-rotation synthesis in the perpendicular direction. The median minor-axis formal uncertainty is 10 μarcseconds, while the median major-axis uncertainty is 312 μarcseconds. In order to properly weight the data set when doing a combined fit with previous astrometry and radial velocity data, we fit an orbital model to the PHASES astrometry by itself, and rescaled the formal uncertainties so as to yield a reduced χ^2 of unity; the resulting scale factor was 2.5, indicating a substantial amount of excess scatter beyond the internal error estimates. We do not believe this scatter to be due to the effect of starspots, given that the *Hipparcos* photometry of this system indicates a scatter of no more than 5 mmag; the resulting maximum starspot-induced astrometric noise would be $\sim 4\mu$arcseconds (Muterspaugh et al. 2006a). We have however identified possible instrumental sources of this systematic error and developed methods for reducing it, see **?**. Nevertheless, the existing astrometry is sufficient to detect astrometric motion induced by the short-period subsystems.

2.2. *Previous Astrometry*

In addition to our astrometry, 88 Tau A has been followed by a number of observers using speckle-interferometric techniques. We use 20 observations tabulated in the *4th Catalog of Interferometric Measurements of Binary Stars*[8] (Hartkopf et al. 2001) to further constrain our fit. Although of somewhat lower precision, the considerable time-baseline (including observations dating from 1985) help constrain the parameters of the wide orbit. In many cases the published astrometry lacks uncertainties, and hence we derive uncertainties from the scatter of the data about a best-fit model. We find the average uncertainty in separation to be 5 milli-arcseconds, and the average position-angle uncertainty to be 3 degrees.

2.3. *Spectroscopic observations and reductions*

From 1984 January through 2006 September we obtained 82 spectrograms of 88 Tau with the Kitt Peak National Observatory (KPNO) 0.9 m coudé feed telescope, coudé spectrograph, and a TI CCD detector. Fifty-eight spectrograms are centered in the red at 6430 Å, cover a wavelength range of about 80 Å, and have a two pixel resolution of 0.21 Å. Those spectra have signal-to-noise ratios of ∼250. The remaining 14 spectrograms are centered in the blue at 4500 Å, cover a wavelength range of 85 Å, and have a resolution of 0.22 Å. Signal-to-noise ratios of ∼300 are typical.

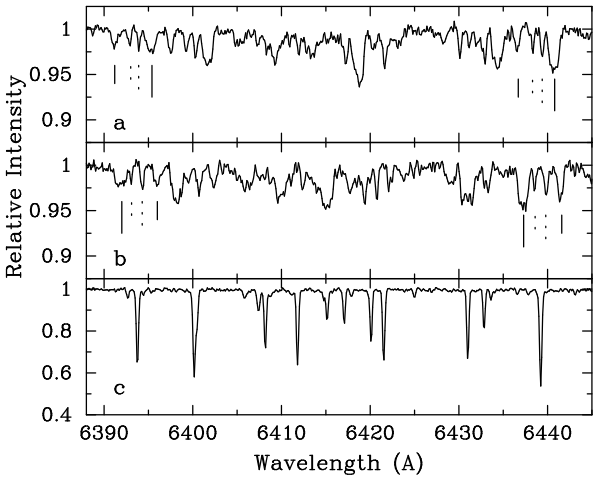

FIG. 2.— Two spectra of 88 Tau, (a) JD 2,452,539.97 and (b) JD 2,454,006.01, compared with (c) the spectrum of the IAU radial velocity standard 10 Tau. The four components of 88 Tau are identified for two different lines. Solid tick marks indicate lines of the 3.57 day binary with the longer tick mark identifying the primary. Dotted tick marks indicate lines of the 7.89 day binary with the longer tick mark identifying the primary.

From 2004 January through 2007 April we acquired 29 spectrograms with the Tennessee State University 2 m automatic spectroscopic telescope (AST), fiber-fed echelle spectrograph, and a 2048 x 4096 SITe ST-002A CCD. The echelle spectrograms have 21 orders, covering the wavelength range 4920–7100 Å with an average resolution of 0.17 Å. The typical signal-to-noise ratio is ∼50. Eaton & Williamson (2004) have given a more extensive description of the telescope, situated at Fairborn Observatory near Washington Camp in the Patagonia Mountains of southeastern Arizona, and its operation.

For the KPNO spectrograms we determined radial velocities with the IRAF cross-correlation program FXCOR (Fitzpatrick 1993), fitting Gaussian functions to the individual cross-correlation peaks. In some cases double Gaussian fits were required to blended cross-correlation peaks. The IAU radial velocity standard star 10 Tau was used as the cross-correlation reference star for the red-wavelength spectrograms. Its velocity of 27.9 km s^{-1} was adopted from Scarfe et al. (1990). Lines in the wavelength region redward of 6445 Å are not particularly suitable for measurement because most features are blends, and there are a number of modest strength water vapor lines. Thus, the radial velocities were determined from lines in the region 6385–6445 Å. However, this 60 Å portion of the spectrum is so small that a spectrum mismatch, caused by the varying strength of line blends with temperature, between the A and F spectral type components of 88 Tau and the F9 IV-V (Keenan & McNeil 1989) spectral type of the reference star 10 Tau, can significantly alter the measured velocity. Thus, in-

[8] `http://ad.usno.navy.mil/wds/int4.html`

TABLE 1
PHASES Astrometric data for for 88 Tau A

HJD-2400000.5	ΔRA (mas)	ΔDec (mas)	σ_{min} (μas)	σ_{maj} (μas)	ϕ_e (deg)	σ_{RA} (μas)	σ_{Dec} (μas)	$\frac{\sigma^2_{RA,Dec}}{\sigma_{RA}\sigma_{Dec}}$	N
52979.34108	-32.1751	-101.5913	20.6	477.9	163.71	458.8	135.5	-0.98733	2353
53034.13365	-40.3179	-91.5425	14.0	311.9	152.78	277.4	143.2	-0.99394	2951
53250.50169	-65.6825	-53.5438	40.2	1775.4	147.24	1493.2	961.3	-0.99876	1027
53271.46723	-70.0370	-48.2688	16.6	669.7	150.15	580.9	333.7	-0.99836	4005
53291.40191	-71.5816	-44.8765	88.3	1759.4	148.37	1498.7	925.8	-0.99371	408
53294.47661	-71.0249	-44.6002	32.3	1700.7	164.09	1635.6	467.2	-0.99742	1355
53312.38113	-74.1285	-40.9475	7.8	68.0	154.15	61.3	30.5	-0.95879	8150
53320.33408	-74.5082	-39.6052	40.3	2076.1	150.23	1802.1	1031.5	-0.99899	1838
53340.29304	-77.4848	-35.5088	18.2	215.1	152.98	191.8	99.1	-0.97862	3602
53341.28228	-77.5104	-35.2746	17.2	551.5	150.70	481.0	270.3	-0.99734	3630
53605.52764	-104.7426	15.6166	18.3	956.5	147.64	808.1	512.1	-0.99911	2855
53606.51559	-106.5080	16.8975	15.7	972.4	146.14	807.5	542.0	-0.99939	3205
53614.50698	-105.6799	17.1892	25.4	773.7	147.94	655.8	411.2	-0.99735	1716
53687.37864	-112.2999	31.2082	24.7	227.4	31.80	193.7	121.7	0.97114	3260
53711.29715	-114.6779	35.8970	80.7	880.5	29.41	768.1	438.0	0.97743	833
53712.28437	-114.0278	36.0764	41.2	326.1	27.87	288.9	156.8	0.95491	2889
53789.14419	-120.0382	51.3801	59.4	3107.9	40.17	2375.3	2005.2	0.99925	761
53790.13775	-119.0373	52.0709	77.5	2663.3	39.39	2058.8	1691.3	0.99824	624
54030.46119	-135.6408	94.2582	50.4	1514.6	163.75	1454.1	426.6	-0.99240	1268
54055.38631	-136.2430	98.5452	48.0	870.1	161.74	826.4	276.5	-0.98318	1679
54061.37247	-136.6968	99.4972	16.3	302.1	163.08	289.0	89.3	-0.98165	4216
54075.33188	-136.8574	101.6204	13.6	250.1	162.18	238.2	77.7	-0.98300	5902
54083.30564	-137.8524	103.1506	31.6	688.5	161.39	652.6	221.8	-0.98863	3845
54084.31595	-136.7985	103.1084	63.9	1741.5	163.11	1666.5	509.6	-0.99139	1182
54103.25456	-137.6742	106.3338	42.7	1011.9	162.34	964.3	309.6	-0.98949	743
54138.15348	-139.3256	112.2494	28.6	457.9	161.38	434.1	148.7	-0.97916	3142

Note. — All quantities are in the ICRS 2000.0 reference frame. The uncertainty values presented in these data have been scaled by a factor of 2.5 over the formal (internal) uncertainties for each night. Column 6 (ϕ_e) is the angle between the major axis of the uncertainty ellipse and the right ascension axis, measured from increasing differential right ascension through increasing differential declination. N is the number of scans obtained in a night; each scan typically represents 0.5–1 second of integration.

stead of cross-correlating this entire 60 Å wavelength region, only the wavelength regions around two or three of the strongest and least-blended lines, usually the Fe I lines at 6394 and 6412 Å plus the Ca I line at 6439 Å, were cross-correlated.

At blue wavelengths the Am star dominates the spectrum. To compute velocities from those spectrograms, 68 Tau, spectral type A2 IV (Abt & Morrell 1995), which has a velocity of 39.0 km s^{-1} (Fekel 1999), was used as the reference star. The region between 4485 and 4525 Å was cross correlated. Resulting velocities are given in Table 2.

For the Fairborn Observatory AST spectra lines in approximately 100 regions, centered on the rest wavelengths (Moore et al. 1966) of relatively strong lines (mostly of Fe I and Fe II) that were not strong blends, were measured. Lines at the ends of each echelle order were excluded because of their lower signal-to-noise ratios. A Gaussian function was fitted to the profile of each component. In some cases a double Gaussian was required to represent blended components. The difference between the observed wavelength and that given in the solar line list of Moore et al. (1966) was used to compute the radial velocity, and a heliocentric correction was applied. The final mean velocity for each observation is given in Table 1. Unpublished velocities of several IAU standard stars with F dwarf spectral types indicate that the Fairborn Observatory velocities have a small zero-point offset of -0.3 km s^{-1} relative to the velocities of Scarfe et al. (1990). Resulting velocities are given in Table 3.

2.4. *Preliminary spectroscopic analysis*

In a study of lithium in Am stars Burkhart & Coupry (1988) acquired two high-resolution spectrograms of 88 Tau in the 6710 Å region. Comparing two sets of lines in the two spectra, they reported detecting the lines of 5 different components. Figure 2 presents two spectra of 88 Tau A in the 6430 Å region that show the two components of the 3.57 day binary near opposite nodes in their spectroscopic orbit, when the components have their maximum velocity separation. Between the two "outside" lines are two additional weak components. From a careful inspection of our KPNO spectra, as well as the ones obtained at Fairborn Observatory, we find lines of only 4 components rather than the 5 reported by Burkhart & Coupry (1988). In Figure 2 many lines of the Am star are ∼5% deep, while the lines of the other 3 components typically have line depths ≤2.5%. Correctly identifying components in such a weak-lined and complex spectrum is not easy because in many spectra two or more of the components are blended.

While the identification of the components of the 3.57 day binary is straightforward, the very weak lines of the other two components are similar enough in strength and line width, making it difficult to tell them apart. To determine a preliminary orbital period, we initially examined only the latter portion of our KPNO velocities, obtained from MJD 50400 to 54000. For each observation we computed the absolute value of the velocity differ-

TABLE 2
KNPO Radial Velocity data for for 88 Tau A

HJD-2400000.5	V_{Aa1} ($km\,s^{-1}$)	Weight[a]	V_{Aa2} ($km\,s^{-1}$)	Weight[b]	V_{Ab1} ($km\,s^{-1}$)	Weight[c]	V_{Ab2} ($km\,s^{-1}$)	Weight[d]
45718.827	91.4	1.0	-66.5	1.0	-	-	-	-
46388.889	-48.7	1.0	141.6	1.0	40.1	1.0	1.1	1.0
46390.712	99.8	1.0	-85.2	1.0	-5.8	1.0	-	-
46718.973	96.5	1.0	-93.7	1.0	59.8	0.4	-4.5	1.0
46720.987	-51.6	1.0	139.5	1.0	-	-	-	-
47152.690	-45.3	1.0	123.6	1.0	57.9	1.0	-	-
47245.612	-50.2	1.0	131.5	1.0	-	-	-	-
47456.764	-52.2	1.0	129.7	1.0	9.3	1.0	-	-
47556.598	-57.7	1.0	135.8	1.0	-	-	-	-
47624.600	-53.5	1.0	125.7	1.0	-	-	-	-
47626.645	66.5	1.0	-57.7	1.0	-	-	4.3	1.0
47627.623	-49.3	1.0	118.9	1.0	-	-	-	-
48345.623	-60.5	1.0	133.2	1.0	-	-	-	-
48347.603	96.5	1.0	-102.4	1.0	9.4	1.0	69.9	0.4
48356.600	-58.6	1.0	128.6	1.0	10.0	1.0	59.1	1.0
48506.018	-46.5	1.0	106.1	1.0	14.0	1.0	53.0	1.0
48573.907	-49.1	1.0	112.7	1.0	42.5	0.4	26.2	0.4
48604.784	90.2	1.0	-98.1	1.0	57.7	0.4	15.4	1.0
48607.806	75.8	1.0	-74.8	1.0	3.0	1.0	-	-
48913.912	-43.0	1.0	105.6	1.0	19.0	1.0	50.9	1.0
48916.875	-55.5	1.0	125.2	1.0	-	-	-	-
49246.972	76.6	1.0	-67.1	1.0	6.6	0.4	-	-
49249.025	-56.1	1.0	131.7	1.0	44.0	1.0	15.3	1.0
49251.037	101.6	1.0	-93.6	1.0	58.9	0.4	1.7	1.0
49302.918	-53.7	1.0	132.4	1.0	12.9	1.0	51.9	1.0
49307.874	91.3	1.0	-87.2	1.0	23.0	0.4	34.6	0.4
49618.936	94.0	1.0	-92.1	1.0	-	-	-	-
49622.925	60.6	1.0	-41.1	1.0	-	-	-	-
49677.881	-50.0	1.0	132.6	1.0	-	-	-	-
49972.035	93.8	1.0	-78.7	1.0	-9.8	1.0	53.5	0.4
49973.934	-48.2	1.0	138.8	1.0	-	-	-	-
49974.035	-51.1	1.0	142.9	1.0	17.0	0.4	26.0	0.4
50365.009	102.5	1.0	-85.3	1.0	5.8	0.4	30.0	0.4
50366.871	-48.5	1.0	146.0	1.0	-	-	-	-
50400.892	100.7	1.0	-88.4	1.0	38.2	1.0	-1.3	1.0
50404.770	91.1	1.0	-66.5	1.0	-	-	-	-
50721.923	93.8	1.0	-67.1	1.0	-9.9	1.0	38.0	0.4
50722.001	96.1	1.0	-77.1	1.0	-11.3	1.0	40.2	1.0
50755.960	-46.1	1.0	139.7	1.0	38.8	1.0	-11.3	0.4
50757.884	104.0	1.0	-86.7	1.0	34.0	1.0	-2.7	1.0
50832.793	104.7	1.0	-82.2	1.0	-9.7	1.0	44.2	1.0
50833.656	57.7	1.0	-	-	-	-	-	-
51088.884	-7.6	1.0	92.2	1.0	-	-	-	-
51089.981	106.0	1.0	-85.2	1.0	-	-	-	-
51091.927	-49.1	1.0	149.9	1.0	-18.8	0.4	47.3	1.0
51093.843	103.8	1.0	-79.4	1.0	3.6	0.4	22.0	0.4
51473.877	-51.8	1.0	147.2	1.0	43.5	1.0	-18.3	0.4
51475.781	107.5	1.0	-85.7	1.0	-	-	-	-
51475.862	107.8	1.0	-85.7	1.0	22.1	0.4	4.1	0.4
51803.989	95.8	1.0	-66.7	1.0	-	-	-	-
51805.963	-49.1	1.0	147.2	1.0	41.6	1.0	-21.2	0.4
51807.963	107.0	1.0	-86.9	1.0	5.1	0.4	22.7	0.4
52016.610	-46.8	1.0	142.6	1.0	-	-	-	-
52180.962	-49.0	1.0	146.2	1.0	-14.7	1.0	43.8	1.0
52182.981	104.0	1.0	-86.2	1.0	28.2	0.4	0.4	0.4
52327.604	-48.8	1.0	145.5	1.0	35.9	1.0	-0.9	0.4
52329.648	89.8	1.0	-64.0	1.0	-8.0	0.4	38.2	0.4
52537.994	-50.0	1.0	137.7	1.0	35.0	1.0	-4.0	0.4
52539.968	106.0	1.0	-89.1	1.0	42.9	1.0	-7.0	1.0
52541.878	-46.3	1.0	144.8	1.0	-	-	-	-
52541.973	-45.5	1.0	139.3	1.0	1.5	0.4	38.9	1.0
52705.698	-45.8	1.0	126.6	1.0	48.5	1.0	-	-
52707.690	101.6	1.0	-88.8	1.0	-	-	-	-
52709.627	-54.6	1.0	144.6	1.0	-	-	51.1	1.0
52903.938	93.6	1.0	-75.7	1.0	-	-	-	-
52941.845	-50.8	1.0	141.1	1.0	51.1	1.0	-6.8	0.4
53273.979	-53.1	1.0	139.3	1.0	41.0	1.0	7.9	1.0
53278.990	93.6	1.0	-84.9	1.0	-	-	-	-
53637.954	-55.3	1.0	134.5	1.0	12.9	1.0	42.4	1.0
54001.954	-42.5	1.0	113.7	1.0	3.6	0.4	66.6	1.0
54003.923	89.9	1.0	-90.3	1.0	-	-	-	-
54005.851	-58.5	1.0	137.5	1.0	62.1	1.0	-	-
54006.006	-57.7	1.0	134.6	1.0	60.4	1.0	0.9	0.4

[a]An observation of Aa1 of unit weight has a standard error of 2.0 $km\,s^{-1}$.
[b]An observation of Aa2 of unit weight has a standard error of 2.3 $km\,s^{-1}$.
[c]An observation of Ab1 of unit weight has a standard error of 2.6 $km\,s^{-1}$.
[d]An observation of Ab2 of unit weight has a standard error of 2.6 $km\,s^{-1}$.

TABLE 3
Fairborn Observatory Radial Velocity data for for 88 Tau A

HJD-2400000.5	V_{Aa1} ($km\,s^{-1}$)	Weight[a]	V_{Aa2} ($km\,s^{-1}$)	Weight[b]	V_{Ab1} ($km\,s^{-1}$)	Weight[c]	V_{Ab2} ($km\,s^{-1}$)	Weight[d]
53020.704	-38.5	1.0	118.0	1.0	50.8	1.0	-	-
53032.697	101.1	1.0	-90.3	1.0	-6.3	1.0	53.7	1.0
53052.773	-43.0	1.0	126.0	1.0	50.9	1.0	-	-
53276.989	-37.3	1.0	110.0	1.0	-	-	53.0	1.0
53285.968	85.9	1.0	-69.9	1.0	10.8	1.0	41.8	1.0
53314.892	102.0	1.0	-95.0	1.0	8.8	1.0	40.6	1.0
53350.890	93.6	1.0	-85.3	1.0	46.3	1.0	7.7	1.0
53395.775	-28.2	1.0	97.3	1.0	-2.4	1.0	58.0	1.0
53405.684	-44.4	1.0	127.0	1.0	39.9	1.0	11.9	1.0
53631.018	-55.6	1.0	139.5	1.0	2.7	1.0	57.9	1.0
53644.977	-48.0	1.0	127.2	1.0	38.3	1.0	20.1	1.0
53659.986	-33.5	1.0	102.9	1.0	58.4	1.0	-	-
53700.887	90.5	1.0	-82.3	1.0	-	-	-	-
53741.743	-56.5	1.0	139.1	1.0	-1.2	1.0	56.7	1.0
54191.632	-61.0	1.0	136.8	1.0	7.3	1.0	63.7	1.0
54194.634	-28.7	1.0	85.1	1.0	-	-	-	-
54194.656	-30.2	1.0	89.5	1.0	-	-	-	-
54198.610	-56.9	1.0	132.4	1.0	-	-	-	-

[a]An observation of Aa1 of unit weight has a standard error of 2.0 $km\,s^{-1}$.
[b]An observation of Aa2 of unit weight has a standard error of 2.3 $km\,s^{-1}$.
[c]An observation of Ab1 of unit weight has a standard error of 2.6 $km\,s^{-1}$.
[d]An observation of Ab2 of unit weight has a standard error of 2.6 $km\,s^{-1}$.

ence between the two components and then used those results as the input data for two different period finding approaches. First, a sine curve was fitted to the velocity differences for trial periods between 1 and 100 days with a step size of 0.0005 days. The period with the smallest sum of the squared residuals was adopted as the best period. Next, a search over a similar period range and with the same step size was done with the least string method (Bopp et al. 1970). Both searches resulted in a period of 3.9435 days. Doubling this period produced an orbital period of 7.887 days. Separate analyses of our earlier KPNO velocities as well as the Fairborn Observatory velocities produced a similar orbital period. We then adopted the 7.887 day period and computed a phase diagram to identify correctly the components. Afterward we compared those results with an attempt at visual identification, based on which set of lines appeared to be stronger in each spectrum. The visual inspection correctly identified the more massive component only about half of the time. Apparently, the lines of these two components are similar enough that weak lines from other components and noise can significantly affect the apparent line strengths. Thus, we conclude that it is not possible to differentiate the two components based on line strength.

2.5. *Orbital Models*

In modeling the hierarchical quadruple system we make the simplifying assumption that the three orbital systems do no perturb each other during the time of our observations, i.e. we use three Keplerian orbital systems, one wide (Aa-Ab) and slow (18-year period), and two short period systems: Aa1-Aa2, 3.57-day period, and Ab1-Ab2, 7.89-day period. Note that one cannot simply superimpose the separation vectors from the three models; this is because the PHASES observable is the angle between the two Centers-of-Light (COL) of the short-period systems.

$$\begin{aligned}\overrightarrow{y_{\rm obs}} = & \overrightarrow{r_{\rm Aa-Ab}} \\ & + \frac{R_A - L_A}{(1+R_A)\,(1+L_A)} \overrightarrow{r_{\rm Aa1-Aa2}} \\ & - \frac{R_B - L_B}{(1+R_B)\,(1+L_B)} \overrightarrow{r_{\rm Ab1-Ab2}} \end{aligned} \quad (1)$$

Here $R_A = M_{\rm Aa2}/M_{\rm Aa1}$ is the Aa component mass ratio and $L_A = L_{\rm Aa2}/L_{\rm Aa1}$ the luminosity ratio, while $R_B = M_{\rm Ab2}/M_{\rm Ab1}$ and $L_B = L_{\rm Ab2}/L_{\rm Ab1}$ are the corresponding rations for the Ba–Bb sub-system. Including this coupling term for astrometric data is important when a full analysis including radial velocity data is made.

3. RESULTS

The best-fit orbital model was found using an iterative non-linear least-squares minimization scheme. The best-fit parameters are found in Table 4. The reduced χ_r of the combined fit to PHASES, radial velocity, and previous differential astrometry data is 1.37. This combined set has 378 data points (49 of which are two-dimensional astrometric points) and 37 free parameters. The fits to the astrometric and radial-velocity data for the various subsystems are shown in Figures 3–7. We find that the two short-period systems have eccentricities consistent with zero, and we therefore held these parameters fixed at zero for the fit. The time of maximum primary apparent velocity is chosen as zero orbital phase.

TABLE 4
Best-fit Orbital Parameters for 88 Tau A

Parameter	Value	Uncertainty
χ^2	547	
χ_r	1.37	
No.Param.	37	
$P_{\rm AaAb}$(days)	6585.90	±12
$e_{\rm AaAb}$	0.0715	±0.0026
$i_{\rm AaAb}$(deg.)	69.9228	±0.048
$\omega_{\rm AaAb}$(deg.)	205.7	±1.2
$T_{\rm AaAb}$(HMJD)	55261.7	±22
$\Omega_{\rm AaAb}$(deg.)	146.734451	±0.067
$M_{\rm Aa}(M_\odot)$	3.42	±0.18
$M_{\rm Ab}(M_\odot)$	2.13	±0.13
d(pc)	50.70	±0.88
$P_{\rm Aa1Aa2}$(days)	3.571096	±0.000003
$e_{\rm Aa1Aa2}$	0.0	*N/A*
$i_{\rm Aa1Aa2}$(deg.)	110.6	±2.7
$\omega_{\rm Aa1Aa2}$(deg.)	0.0	*N/A*
$T_{\rm Aa1Aa2}$(HMJD)	53389.3824	±0.0030
$\Omega_{\rm Aa1Aa2}$(deg.)[a]	287.5	±1.8
$M_{\rm Aa2}/M_{\rm Aa1}$	0.6602	±0.0028
$L_{\rm Aa2}/L_{\rm Aa1}$(K-band)[a]	0.249	±0.035
$P_{\rm Ab1Ab2}$(days)	7.886969	±0.000066
$e_{\rm Ab1Ab2}$	0.0	*N/A*
$i_{\rm Ab1Ab2}$(deg.)	27.23	±0.72
$\omega_{\rm Ab1Ab2}$(deg.)	0.0	*N/A*
$T_{\rm Ab1Ab2}$(HMJD)	52507.31	±0.02
$\Omega_{\rm Ab1Ab2}$(deg.)[b]	34.0	±8.2
$M_{\rm Ab2}/M_{\rm Ab1}$	0.988	±0.024
$L_{\rm Ab2}/L_{\rm Ab1}$(K-band)[b]	0.865	±0.028
V_0(KNPO, km s^{-1})	23.70	±0.17
V_0(Fairborn, km s^{-1})	23.91	±0.31

[a] An alternate, but disfavored, solution has $L_{Aa2}/L_{Aa1} = 1.48$ and $\Omega_{Aa1Aa2} = 326$.
[b] An alternate solution has $L_{Ab2}/L_{Ab1} = 1.10$ and $\Omega_{Ab1Ab2} = 205$.

3.1. *Relative Orbital Inclinations*

The mutual inclination Φ of two orbits is given by

$$\cos\Phi = \cos i_1 \cos i_2 + \sin i_1 \sin i_2 \cos(\Omega_1 - \Omega_2) \quad (2)$$

where i_1 and i_2 are the orbital inclinations and Ω_1 and Ω_2 are the longitudes of the ascending nodes. For this quadruple system we derive three separate mutual inclinations, corresponding to the three possible pairwise comparisons of the three orbits in this system (i.e. $Aab - Aa1Aa2$, $Aab - Ab1Ab2$ and $Aa1Aa2 - Ab1Ab2$). The resulting values found from our combined orbital solutions are given in Table 5.

It should be noted that even with both COL-astrometry and radial-velocity data, there exists a parameter degeneracy corresponding to an exchange of the ascending and descending nodes together with a change in the luminosity ratio (interchanging which is the brighter star). Given one solution for the mass and luminosty ratios (R_1 and L_1), the other possible luminosity ratio can be found from

$$L_2 = \frac{2R + RL_1 - L_1}{1 + 2L_1 - R} \quad (3)$$

In a quadruple stellar system such as 88 Tau there are 4 possible model solutions. However, as can be seen in Fig.

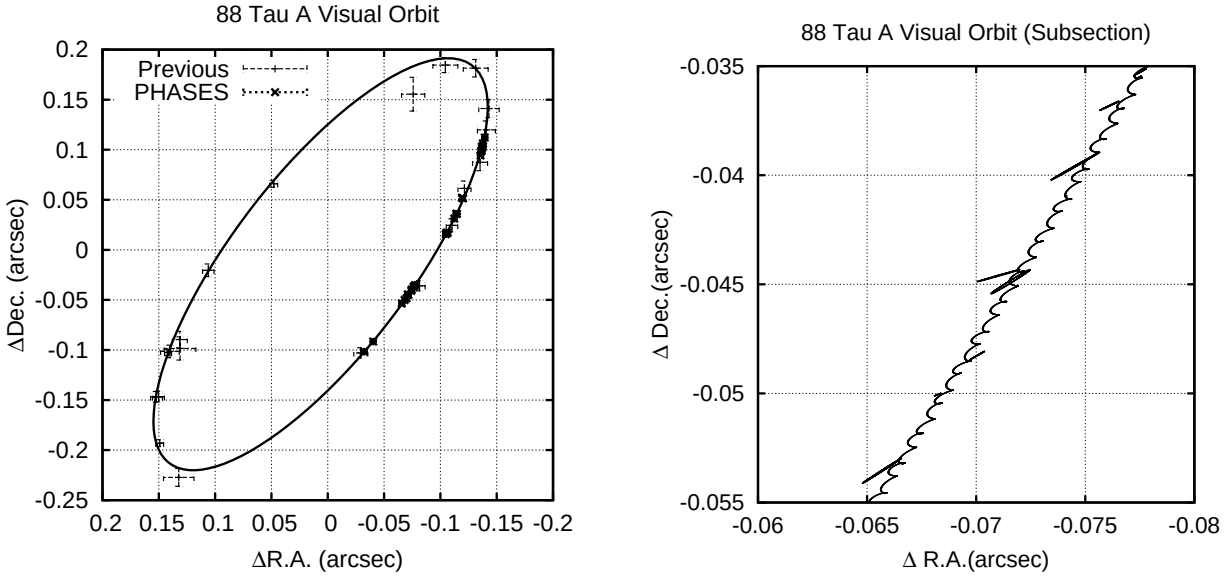

FIG. 3.— (left)The best-fit visual orbit of the 88 Tau Aa-Ab system, together with previously available astrometric data, and our PHASES astrometry. (right) A close-in view of a subsection of the astrometry.

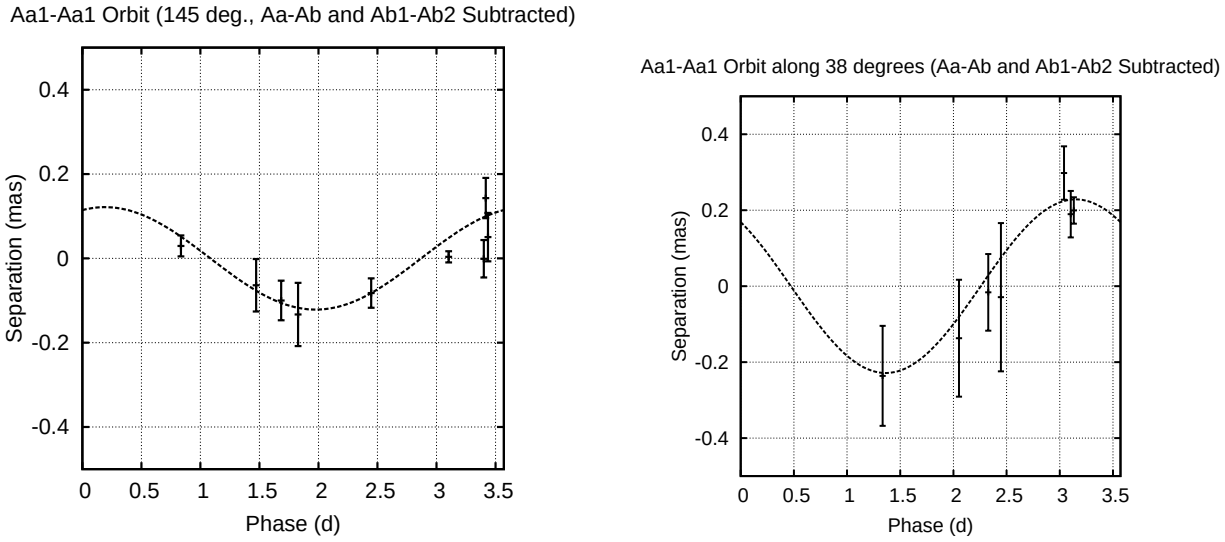

FIG. 4.— The astrometric orbit of the 88 Tau Aa1-Aa2 subsystem, with projected along two different axes (145 degrees East of North deg on the left, 30 degrees on the right.) In each case the motion of the Aa–Ab and other sub-system has been removed. The axes correspond to the two most common orientations of the minor axis of the positional error ellipses (which vary slight from night to night, and between baselines). For clarity, only those observations where the projected uncertainty is less than 300 μas have been included in the plot (all observations are included in the fit).

2 the luminosity of the $Aa1$ component is clearly greater than the $Aa2$ component, hence we choose the solution where $L_{Aa1Aa2} = 0.24$. However, given the nearly-equal masses of the $Ab1$ and $Ab2$ components, it is not entirely clear which is the preferred solution ($L_{Ab1Ab2} = 0.87$ or 1.13, and we calculate the two possible values for the corresponding mutual inclinations.)

The mutual inclination values are above the limit for inclination-eccentricity oscillations derived by (ref kozai).

3.2. *Component Masses and Distance*

This study represents the first determination of the orbital inclinations in this system, and hence the first time the masses have been determined; the precision achieved is $\sim$ 5% for the Aa components and $\sim$ 6 % for the Ab components. The parallax is found to be 19.73 ± 0.34 mas (1.7% uncertainty), placing the system a a greater distance than estimated by *Hipparcos* (21.68 ± 0.82 mas). Our greater distance does however resolve the mass/luminosity discrepancy pointed out by Balega et al. (1999), which arises if one assumes the *Hipparcos* distance to this system.

3.3. *Component Luminosities*

As part of the combined astrometric and radial velocity fit we can solve for the K-band luminosity ratios of the components; this is because the distance and subsystem total masses are essentially determined by the observations of the wide Aa–Ab system, while the subsystem mass ratios are found from the subsystem radial

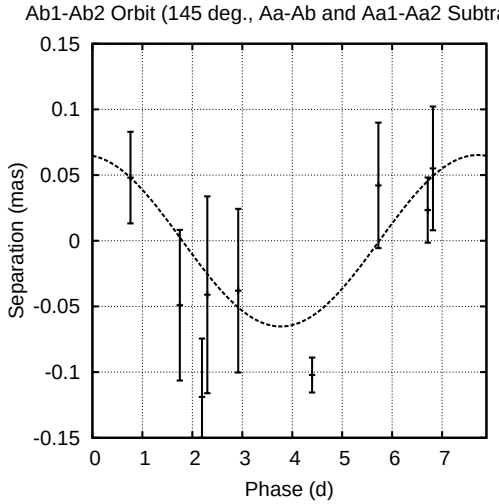

FIG. 5.— The astrometric orbits of the 88 Tau Ab1-Ab2 subsystem. The motion of the Aa–Ab and other sub-system has been removed. The separations shown are projected along an axis oriented 145 degrees East of North, corresponding to mean orientation of the minor axis of the positional error ellipses (which vary slight from night to night). For clarity, only those observations where the projected uncertainty is less than 300 μas have been included in the plot (all observations are included in the fit).

TABLE 5
DERIVED SYSTEM PARAMETERS FOR 88 TAU A

Parameter	Value	Uncertainty
$\Phi_{\rm AaAb-Aa1Aa2}$(deg.)	143.3	±2.5
$\Phi_{\rm AaAb-Ab1Ab2}$(deg.)	82.0[a]	±3.3
$\Phi_{\rm Aa1Aa2-Ab1Ab2}$(deg.)	115.8[b]	±4.6
π(asec)	0.01973	±0.00034
$a_{\rm AaAb}$(milliarcsec)	240.1	±5.3
$a_{\rm Aa1Aa2}$(milliarcsec)	1.35911	±0.034
$a_{\rm Aa1Aa2,col}$(milliarcsec)	0.2696	±0.032
$a_{\rm Ab1Ab2}$(milliarcsec)	1.967	±0.054
$a_{\rm Ab1Ab2,col}$(milliarcsec)	0.065	±0.020
$a_{\rm AB}$(AU)	12.17	±0.17
$a_{\rm Aa1Aa2}$(AU)	0.0689	±0.0012
$a_{\rm Ab1Ab2}$(AU)	0.0997	±0.0021
$K_{\rm Aa}$(km s^{-1})	7.26	±0.38
$K_{\rm Ab}$(km s^{-1})	11.68	±0.42
$K_{\rm Aa1}$(km s^{-1})	78.118	±2.6
$K_{\rm Aa2}$(km s^{-1})	118.326	±3.3
$K_{\rm Ab1}$(km s^{-1})	31.280	±1.4
$K_{\rm Ab2}$(km s^{-1})	31.655	±1.4
$M_{\rm Aa1}$($M_\odot$)	2.06	±0.11
$M_{\rm Aa2}$($M_\odot$)	1.361	±0.073
$M_{\rm Ab1}$($M_\odot$)	1.069	±0.069
$M_{\rm Ab2}$($M_\odot$)	1.057	±0.068

NOTE. — The parameters derived from the best-fit model values in Table 4 and their uncertainties. "col" refers to the amplitude of the motion of the Center of Light of the subsystem in question. Note that our combined astrometry and radial velocity model fits for the system masses drectly, and hence the radial velocity semi-amplitudes are derived secondary parameters.

[a]An alternate solution has $\Phi_{AaAb-Ab1Ab2} = 58$ deg. if $L_{Ab2}/L_{Ab1} > 1$.

[b]An alternate solution has $\Phi_{Aa1Aa2-Ab1Ab2} = 107$ deg. if $L_{Ab2}/L_{Ab1} > 1$.

velocities; this leaves only the component luminosity ratios dependent on the size of the observed astrometric perturbation.

While PTI cannot provide precise determinations of the total system magnitude m_K or the Aa–Ab system differential magnitude Δm_K, these can be found in the literature. Balega et al. (2001) give $\Delta m_{K'} = 1.29 \pm 0.12$ for the Aa-Ab system.

3.4. *Spectral Classes and v sini*

Strassmeier & Fekel (1990) identified several luminosity-sensitive and temperature-sensitive line ratios in the 6430-6465 Å region. Those critical line ratios and the general appearance of the spectrum were employed as spectral-type criteria. However, for stars that are hotter than about early-G, the line ratios in the 6430 Å region have little sensitivity to luminosity, so only the spectral class of an A or F star can be determined. The luminosity class is found by computing the absolute visual magnitude with the *Hipparcos* or our orbital parallax and comparing that magnitude to evolutionary tracks or a table of canonical values for giants and dwarfs.

The red wavelength spectrum of 88 Tau was compared with those of slowly rotating Am, F and G dwarfs. These reference stars, identified mostly from the lists of Abt & Morrell (1995), Keenan & McNeil (1989), and Fekel (1997), were observed at KPNO with the same telescope, spectrograph, and detector as our spectra of 88 Tau. With a computer program developed by Huenemoerder & Barden (1984) and Barden (1985), various combinations of reference-star spectra were rotationally broadened, shifted in radial velocity, appropriately weighted, and added together in an attempt to reproduce the spectrum of 88 Tau in the 6430 Å region. Abt & Morrell (1995) classified 88 Tau as an Am star with spectral classes of A4, A6, and A7 for the calcium, hydrogen, and metal lines, respectively. Their classification of HR 3526 was identical to that of 88 Tau, so we adopted the spectrum of HR 3526 as the proxy for the primary of the 3.57 day binary, which dominates the spectrum at blue wavelengths and is still the strongest component in our red-wavelength region (Fig. 2). The 3 subclass difference between the calcium K line type and metal line type indicates that this star is a marginal or mild Am star (Abt & Bidelman 1969). A good fit to the lines of the 3.57 day secondary was produced by Procyon, spectral type F5 IV-V (Johnson & Morgan 1953). Lines of the two components in the 7.89 day binary are similar in strength and rotation and were well represented by a spectrum of 70 Vir, spectral type G4 V (Keenan & McNeil 1989). Thus, the spectral classes of the four stars are A6m, F5, G4:, and G4:, where the colon indicates that the spectral class is more uncertain than usual because of the weakness of the lines. The abundances of Procyon and 70 Vir are essentially solar, indicating that the abundances of the components of 88 Tau, except for the Am star, are also close to solar.

The continuum intensity ratio of our best reference star combination, fitted to the spectrum of 88 Tau, is 0.79:0.11:0.05:0.05. If we adopt the continuum intensity ratios as the luminosity ratios at 6430 Å, we obtain a magnitude difference of 2.1 ± 0.3 between the 3.57 day pair, and 2.4 ± 0.3 between the astrometric components, where the uncertainties are estimated. The 6430 Å wavelength is about 0.6 of the way between the center of the Johnson V and R bandpasses.

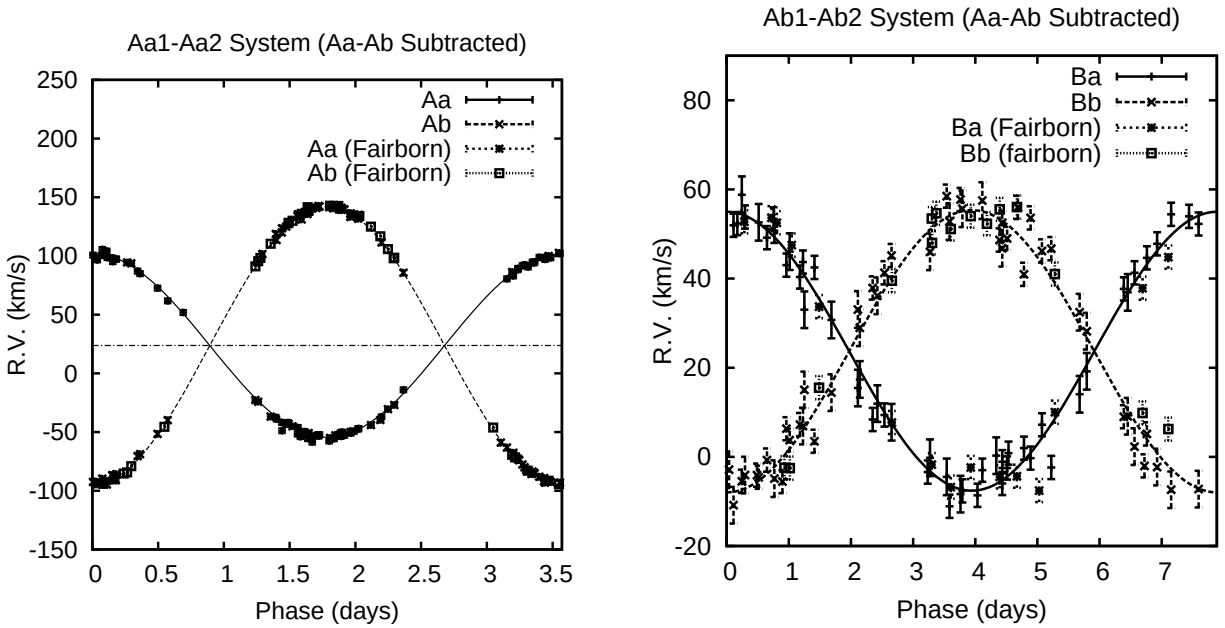

FIG. 6.— (left) The measured and model radial velocities of the Aa1–Aa2 subsystem, phased about the best-fit orbital model, and with the motions due to the Aa–Ab orbit subtracted out. (right) Measured and model radial velocities of the Ab1–Ab2 subsystem, with the Aa--Ab motion removed.

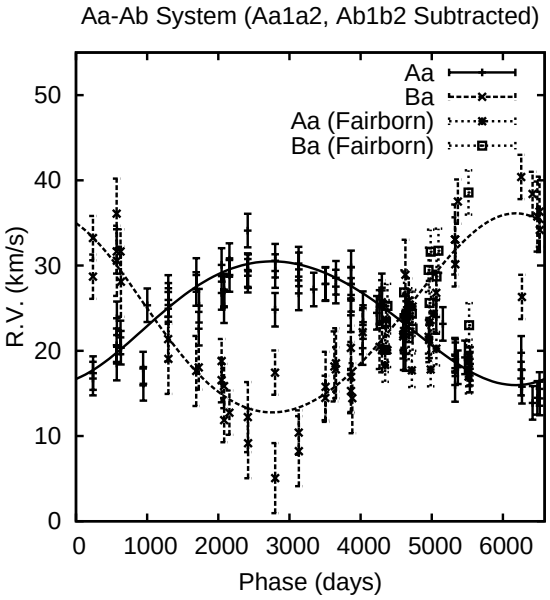

FIG. 7.— The measured and modeled radial velocities of the 88 Tau Aa-Ab system, with the motion due to the Aa1–Aa2 and Ab1–Ab2 systems subtracted.

With the procedure of Fekel (1997), we determined projected rotational velocities for the 4 components of 88 Tau from 10 KPNO red-wavelength spectra. For each spectrum the full-widths at half-maximum of 2 or 3 unblended lines in the 6430 Å region were measured and the results averaged for each component. The instrumental broadening was removed, and the calibration polynomial of Fekel (1997) was used to convert the resulting broadening in angstroms into a total line broadening in km s^{-1}. From Fekel (1997, 2003) we assumed a macroturbulence of 0.0 for the Am star, 4 km s^{-1} for the mid-F star, and 3 km s^{-1} for the G stars. The resulting $v \sin i$ values are 37 ± 2 and 17 ± 2 km s^{-1} for the primary and secondary of the 3.57 day binary, respectively, and 5 ± 3 km s^{-1} for both components of the 7.89 day binary. Our value for the Aa1 component is consistent with the determination of $v \sin i = 36$ km s^{-1} by Royer et al. (2002).

4. CONCLUSION

PHASES interferometric astrometry has been used together with radial velocity data to measure the orbital parameters of the quadruple star system 88 Tau A, and in particular to resolve the apparent orbital motion of the close Aa1-Aa2 and Ab1-Ab2 pairs. For the first time we have determined the Ab system to be spectroscopic binary; the amplitude of the Ab1-Ab2 Center-of-Light motion is only $\sim 65\mu$as, indicating the level of astrometric precision attainable with interferometric astrometry. By measuring both orbits one is able to determine the mutual inclinations of the orbits. We have also been able to determine the component masses and distance to the system with a precision at the few-percent level.

We wish to acknowledge the extraordinary observational efforts of K. Rykoski. Observations with PTI are made possible despite the efforts of the PTI Collaboration, which we acknowledge. This research has made use of services from the Michelson Science Center, California Institute of Technology, http://msc.caltech.edu. Part of the work described in this paper was performed at the Jet Propulsion Laboratory under contract with the National Aeronautics and Space Administration. This research has made use of the Simbad database, operated at CDS, Strasbourg, France, and of data products from the Two Micron All Sky Survey, which is a joint project of the University of Massachusetts and the Infrared Processing and Analysis Center/California Institute of Technology, funded by the NASA and the NSF. We thank T.

Willmitch for measuring some of the early KPNO spectra. The work of FCF and MW has been supported in part by NASA grant NCC5-511 and NSF grant HRD-9706268. PHASES is funded in part by the California Institute of Technology Astronomy Department, and by the National Aeronautics and Space Administration under grant NNG05GJ58G issued through the Terrestrial Planet Finder Foundation Science Program. This work was supported in part by the National Science Foundation through grants AST-0300096 and AST-0507590.

REFERENCES

Abt, H. A., & Bidelman, W. P. 1969, 158, 1091
Abt, H. A., & Morrell, N. I. 1995, ApJS, 99, 135
Barden, S. C. 1985, ApJ, 295, 162
Balega, I. I., Balega, Y. Y., Hofmann, K.-H., Tokovinin, A. A., & Weigelt, G. P. 1999, Astronomy Letters, 25, 797
Balega, I. I., Balega, Y. Y., Hofmann, K.-H., & Weigelt, G. 2001, Astronomy Letters, 27, 95
Boden, A., Creech-Eakman, M., Queloz, D., 2000, ApJ, 536, 880-890.
Bopp, B. W., Evans, D. S., & Laing, J. D. 1970, MNRAS, 147, 355
Burkhart, C., & Coupry, M. F. 1988, A&A, 200, 177
Colavita, M. M.,et al. 1999, ApJ, 510 , 505.
Colavita, M. M., 1999, PASP, 111, 111.
Colavita, M., et al. 2003, ApJ, 592, L83
Cowley, A., Cowley, C., Jaschek, M., & Jaschek, C. 1969, AJ, 74, 375
Cox, A. N., 1999, Allens Astrophysical Quantities, Springer-Verlag, New York.
Eaton, J. A., & Williamson, M. H. 2004, SPIE, 5496, 710
Fekel, F. C. 1997, PASP, 109, 514
Fekel, F. C. 1999, IAU Colloquium 170, Precise Stellar Radial Velocities, eds. J. B. Hearnshaw and C. D. Scarfe (San Francisco: ASP), 378
Fekel, F. C., Joyce, R. R., Hinkle, K. H., & Skrutskie, M. F. 2000, AJ, 119, 1375
Fekel, F. C. 2003, PASP, 115, 807
Fitzpatrick, M. J. 1993, in ASP Conf. Ser. 52, Astronomical Data Analysis Software and Systems II, ed. R. J. Hanisch, R. V. J. Brissenden, & J. Barnes (San Francisco: ASP), 472
Hartkopf, W. I., McAlister, H. A., & Mason, B. D. 2001, AJ, 122, 3480
Huenemoerder, D. P., & Barden, S. C. 1984, BAAS, 16, 510
Johnson, H. L., & Morgan, W. W. 1953, ApJ, 117, 313
Keenan, P. C., & McNeil, R. C. 1989, ApJS, 71, 245
Lane, B. F., & Muterspaugh, M. W. 2004, ApJ, 601, 1129
McAlister, H. A., Hartkopf, W. I., Hutter, D. J., & Franz, O. G. 1987, AJ, 93, 688
Muterspaugh, M. W., Lane, B. F., Konacki, M., Burke, B. F., Colavita, M. M., Kulkarni, S. R., & Shao, M. 2005, AJ, 130, 2866
Muterspaugh, M. W., Lane, B. F., Konacki, M., Burke, B. F., Colavita, M. M., Kulkarni, S. R., & Shao, M. 2006, A&A, 446, 723
Muterspaugh, M. W., Lane, B. F., Konacki, M., Wiktorowicz, S., Burke, B. F., Colavita, M. M., Kulkarni, S. R., & Shao, M. 2006, ApJ, 636, 1020
Muterspaugh, M. W., Lane, B. F., Kulkarni, S. R., Burke, B. F., Colavita, M. M., & Shao, M. 2006, ApJ, 653, 1469
Moore, C. E., Minnaert, M. G. J., & Houtgast, J. 1966, The Solar Spectrum 2935 Å to 8770 Å, National Bureau of Standards Monograph 61 (Washington, D. C.: U. S. Government Printing Office)
Royer, F., Grenier, S., Baylac, M.-O., Gómez, A. E., & Zorec, J. 2002, A&A, 393, 897
Scarfe, C. D., Batten, A. H., & Fletcher, J. M. 1990, Publ. Dominion Astrophy. Obs., 18, 21
Skrutskie, M. F. et al, 2006, AJ, 131, 1163.
Strassmeier, K. G., & Fekel, F. C. 1990, A&A, 230, 389
Sterzik, M. F., & Tokovinin, A. A. 2002, A&A, 384, 1030
Tokovinin, A. A., & Gorynya, N. A. 2001, A&A, 374, 227
Tokovinin, A., Thomas, S., Sterzik, M., & Udry, S. 2006, A&A, 450, 681
Tokovinin, A. A. 1997, A&AS, 124, 75